Influence of an external applied AC magnetic field on the melt pool dynamics at high-power laser beam welding

Influence of an external applied AC magnetic field on the melt pool dynamics at high-power laser beam welding

Ömer Üstündağ[1], Nasim Bakir[1], Andrey Gumenyuk[1,2], Michael Rethmeier[3,1,2]

[1]Bundesanstalt für Materialforschung und -prüfung (BAM), Unter den Eichen 87, 12205 Berlin, Germany
[2]Fraunhofer Institute for Production Systems and Design Technology, Pascalstraße 8-9, 10587 Berlin, Germany
[3]Institute for Machine Tools and Factory Management, Technische Universität Berlin, Pascalstraße 8-9, 10587 Berlin, Germany

oemer.uestuendag@bam.de

Abstract. The study deals with the determination of the influence of an externally applied oscillating magnetic field on the melt pool dynamics in high power laser beam and hybrid laser arc welding processes. An AC magnet was positioned under the workpiece which is generating an upward directed electromagnetic force to counteract the formation of the droplets. To visualise the melt flow characteristics, several experiments were carried out using a special technique with mild steel from S355J2 with a plate thickness of up to 20 mm and a quartz glass in butt configuration. The profile of the keyhole and the melt flow were recorded with a high speed camera from the glass side. Additionally, the influence of the magnetic field orientation to the welding direction on the filler material dilution on laser hybrid welding was studied with variating oscillation frequency. The element distribution over the whole seam thickness wa measured with X-ray fluorescence (XRF). The oscillation frequency demonstrated a great influence on the melt pool dynamics and the mixing of the elements of the filler wire. The high speed recordings showed, under the influence of the magnetic field, that the melt is affected under strong vortex at the weld root, which also avoids the formation of droplets.

1. Introduction

Despite the availability of high-power laser systems within the range beyond 100 kW on the market, the use of high-power laser beam welding (LBW) for thick metal sections at industrial scale are still under discussion. Its application for plate thicknesses greater than 15 mm has certain technological limitations. One of the limiting factors is the formation of sagging due to the gravitational forces or the hydrostatic pressure often observed during welding in flat position (1G). For that reason, the arc-based welding processes are usually implemented for welding of thick-walled structures with wall thicknesses above 15 mm. However, these are less productive as compared with high-power LBW cause of lower penetration depth. Hence, multi-layer technology is used for welding of thick metal plates. It leads to high heat inputs and distortion or thermal induced residual stress of the plates as well as reworks hindrances such as flame straightening thus expend more time and cost.

Several investigations were conducted to identify the maximum boundaries of the single-pass high power LBW or hybrid laser-arc welding (HLAW) and their challenges and physical backgrounds. Similar challenges or defects are to be expected for high-power LBW or HLAW. Single-pass HLAW

was produced up to 28 mm metal thickness using a laser power of just 19 kW with an electromagnetic weld pool support system [1] or HLAW of 25 mm thick plates using cut-wire, which was filled within an air gap between workpieces, with ceramic or flux backing and also up to 50 mm depth by double sided welds approach showed successful outcomes [2]. Multilayer high-power LBW, especially HLAW technique was demonstrated in [3] for one sided steel welds ranging in thickness from 28 mm to 32 mm in two to five layers. Laser beam welding process under vacuum conditions [4,5], laser submerged arc hybrid welding [6], or narrow-gap laser-arc hybrid welding [7] were conducted successfully for deep penetration weld joints. As reported in the studies dealing with single-pass high-power LBW, the formation of sagging or drop-outs is a major challenge during welding. Guidelines for preventing the drop-outs were reported in [8], where the increase of the welding speed or laser power is recommended for the prevention of those defects. The main physical background of this recommendation lies in the fact, that with increasing welding speed the geometrical sizes of the seam is changed to thinner seam width. This leads to the increase of the surface tension which counteracts the hydrostatic pressure on the root part. Hence, the stability criterion is dependent on geometrical dimensions of weld seams and is defined in conformance with [9] as shown in Equation 1:

$$h \times w < 2\, l_{cap}^2, \tag{1}$$

where h is the plate thickness, w is the root width, $l_{cap} = [\gamma/(\rho g_0)]^{1/2}$ is the capillary length, γ is the surface tension coefficient, ρ is the density of the melt, and g_0 is the gravitational acceleration. The geometrical sizes on the root side of the weld pool and the stability criterion for liquid steel is shown in Figure 1 according to [9].

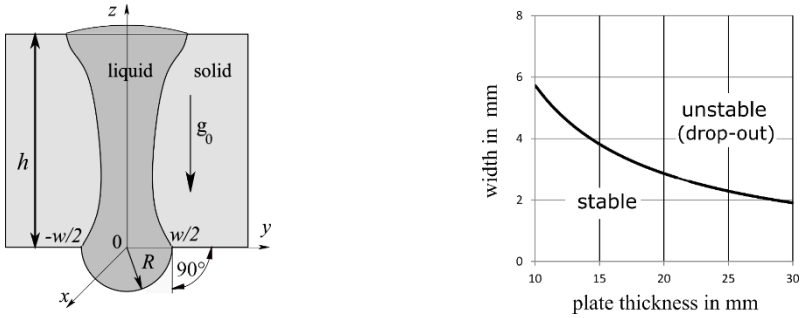

Figure 1. Geometrical sizes on the root side of the weld pool (left) stability criterion for liquid steel (right) [9].

Another typical problem associated with the application of high-power HLAW or wire feed LBW at deep penetration is the inadequate and non-uniform distribution of filler wire elements over the entire seam depth which may deteriorate mechanical properties especially in the root part. The high-power LBW seams are characterized by a high cooling rate, why deteriorated mechanical properties can be observed, especially at LBW of high-strength steels. So, the use of a filler wire and a homogeneous mixing of the filler wire plays an integral role to achieve the required mechanical properties. In [10] it was reported that the Charpy impact toughness of a single-pass hybrid laser-arc welded 25 mm thick structural steel plate is decreased up to 60 % in the root part (laser-dominated zone) compared to the top part (arc-dominated zone). Thereby, the decrease in cooling time over depth, the resulting microstructure and grain size, together with the inhomogeneous mixing have a great impact on the mechanical properties. Studies dealing with the improvement of the dilution are already known. In [11] the influence of the arc mode during HLAW on the dilution was studied, where a pulsed or modified spray modes were recommended. Another effective method to improve the filler wire dilution is to weld thick plates with a small air gap of 0.3 mm to 0.4 mm as reported in [12,13]. The effectiveness of trailing GMAW configuration in the mixing of the melt during the welding of 10 mm thick plates was noted in [14]. The same approach was shown in [15]. Additionally, the shielding gas containing more than 2 % O_2 produces a more homogenous distribution of alloying elements [15]. The impact of the welding parameters such as laser beam power, wire feed speed and resulting arc power, distance between the two heat sources

and the configuration was studied in [16]. It was found that with increasing laser power and arc current, the filler wire mixing was improved. With a distance of 2 mm to 6 mm between the wire tip extension and the laser beam, promising results could be achieved.

As the state-of-the-art shows, the challenges during high-power LBW or HLAW of thick-walled steels, especially the formation of drop-outs and inhomogeneous filler wire mixing is well known. Methods with the adaptation of the welding parameters for the prevention of an inhomogeneous mixing were developed for welds with a thickness of up to 15 mm. For thicker plates an additional external force may be needed to influence the melt flow dynamics for a better mixing behaviour. Therefore, external magnetic fields were applied in some studies such as in [17-21]. A magnet with a low frequency in the range of 10 Hz to 20 Hz was applied for the improvement of the element distribution for LBW of 3 mm thick aluminum plate [17-19]. In [20] an external magnetic field was applied for wire-feed LBW of 10 mm thick austenitic stainless steel to improve the mixing behaviour. It was found that a bulging region is formed, which narrows the metal transfer channel from the top to the bottom region. A change of the magnetic field orientation of 10° to 20° to the welding direction was recommended numerically as well as experimentally to eliminate the bulging phenomenon, thus providing a downward transfer channel for the melt flow. An approach to prevent sagging and to improve the filler wire mixing at single-pass HLAW of steel plates with a wall thickness of 20 mm was demonstrated in [21]. Therefore, an AC magnet was positioned under the workpiece and operated with a frequency of approx. 1.2 kHz.

The goal of this study is to describe the melt flow characteristics in detail and to show the influence of the magnetic field orientation and oscillation frequency on the filler wire mixing during high-power LBW and HLAW.

2. Experimental Setup

2.1. Laser beam welding experiments in steel-glass configuration

The high-power fibre laser IPG YLR-20000 with a maximum output power of 20 kW was used as the laser beam source. The emission wavelength and beam parameter product were 1070 nm and 11 mm x mrad, respectively. The laser radiation was transmitted through an optical fibre with a core diameter of 200 µm. A laser-processing head BIMO HP has been selected, which provides a magnification of 2.8 so that the laser beam can be focused into a spot with a diameter of 560 µm. To detect the keyhole during high-power laser beam welding a special setup was necessary. Welding trials in butt joint configuration of 25 mm thick structural steel plate (S355J2) and quartz glass were conducted. A groove with the dimensions of 80 mm x 8 mm x 0.5 mm was milled on the steel plate and filled with an austenitic powder 316L-Si with Ni as tracing element for the later evaluation. Side views of the molten pool were taken with help of a highspeed camera Fastcam 1024PCI and interference band-pass filter at 808 nm and band width of 20 nm. The frame rate and the frame size were 2000 fps and 1200 pixels to 1200 pixels, respectively. An oscillating magnetic field generated by an AC electromagnet was applied to the root side of the weld specimen, where the magnetic field was perpendicular and induced electric current parallel to the welding direction. The schematic representation of the experimental setup is shown in Figure 2. The LBW experiments on steel-glass configuration were performed using a laser beam power of 18.7 kW at a welding speed of 0.9 m min^{-1} and a focal position of -7 mm. The AC magnet was operated at an oscillation frequency of 1.2 kHz and a magnet power of 2.1 kW ± 200 W. To protect the arc on the top side from a deflection due to the oscillating magnetic field, the frequencies have been selected in the kHz range, where the skin layer depth is less than the plate thickness. For the evaluation of the high-speed recordings the displacements in the melt-glass interface were estimated and then the velocities were calculated using the optical flow algorithm according to Lucas-Kanade method.

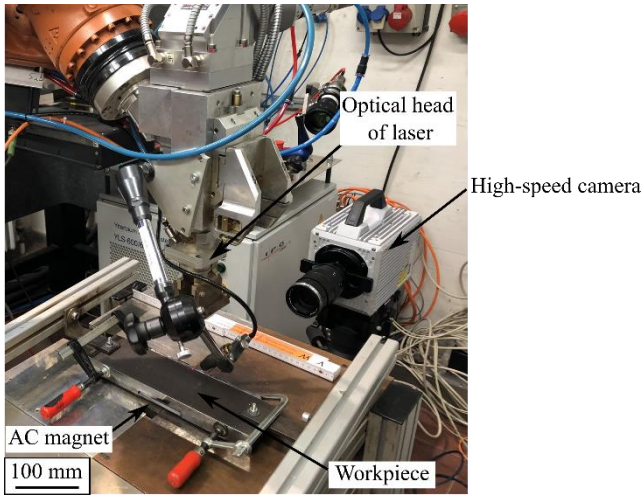

Figure 2. Experimental setup for LBW in steel-glass configuration.

For metallographic inspection, longitudinal sections of the laser beam welded samples were cut. After polishing and etching the samples using 2 % nital solution, the mixing of the powder over the thickness was evident.

2.2. Hybrid laser-arc welding experiments

The HLAW experiments were performed using the same laser source as described in Section 2.1. Additionally, a welding machine Cloos Quineo with a maximum current of 600 A was used as an arc power source. The laser optics and GMAW torch were mounted on the robot arm, where the laser axis was positioned 90° to the weld specimen surface and the GMA torch was tilted 25° relative to the laser axis. The processing head and the magnet remained in a fixed position during the welding, where the specimens were moved by an external axis. The experiments were carried out on 20 mm thick structural steel plates (S355J2) in butt joint configuration with an arc leading position and a distance of 4 mm between the two heat sources and under the following welding parameters: laser beam power of 17.7 kW; welding speed of 1.3 m min^{-1}; focal position of the laser beam of -5 mm; wire feed speed of 13 m min^{-1}; stick-out of 18 mm; shielding gas mixing consisted of 18% CO_2 in Ar with a volume flow rate of 20 m min^{-1}. A Ni-based solid wire Thermanit625 (ERNiCrMo-3 according to AWS A-5.14) with a diameter of 1.2 mm was used as a filler wire. Figure 3 shows the setup for the HLAW experiments. Different magnetic field orientation and oscillating frequencies were tested to determine the influence of the magnetic parameters on the filler wire mixing.

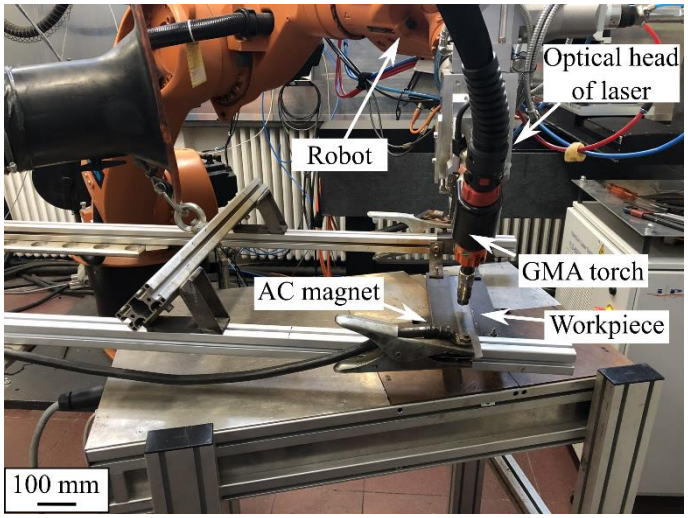

Figure 3. Experimental setup for HLAW of 20 mm thick S355J2 in butt joint configuration with 15°-turn of the magnetic field orientation.

To evaluate the metal mixing, the Ni-content was measured then with the X-ray fluorescence method (XRF) over the whole seam thickness.

2.3. Welding materials

For the experiments structural steel plates of S355J2 with a thickness of 20 mm and 25 mm were used. The filler wire diameter was 1.2 mm. The particle size distribution of the powder was between 53 µm and 106 µm. The chemical composition of the materials used are listed in Table 1.

Table 1. Chemical composition of materials used, shown in wt-%.

Material/Element	C	Mn	Si	P	S	Cr	Ni	Mo	Cu	Nb	Fe
S355J2	0.08	1.3	0.29	0.019	0.004				0.08		bal.
Thermanit 625	0.03	0.2	0.25			22	bal.	9		3.6	< 0.5
316L-Si powder	0.01	0.5	2.1	0.02	0.01	16.9	11.9	3			bal.

3. Results and discussion

3.1. Laser beam welds

The LBW experiments in steel-glass configuration were conducted to observe the prevention of the drop-outs and to evaluate the melt flow characteristic in dependence on the external applied AC magnetic field. First, the magnetic field orientation was unchanged, so that the oscillating magnetic field was perpendicular to the welding direction, while the generated Lorentz force is directed upwards to counteract the hydrostatic pressure. The laser beam was positioned on the front edge of the magnet poles (see Figure 4), so that the drop, which is formed at the rear side of the molten pool is in the middle of the magnet poles, where the magnetic field density is high enough to suppress the drop-out pushing the melt upwards. Figure 4 shows three images of the high-speed records, where the start of the formation of a drop-out (t_0) can be seen clearly. After a time-step of $\Delta t = 5$ ms (10 frames) the volume of the droplet is increased. In the middle of the magnet poles, the electromagnetic pressure compensates the droplet, which is visible on the right-hand side of Figure 4.

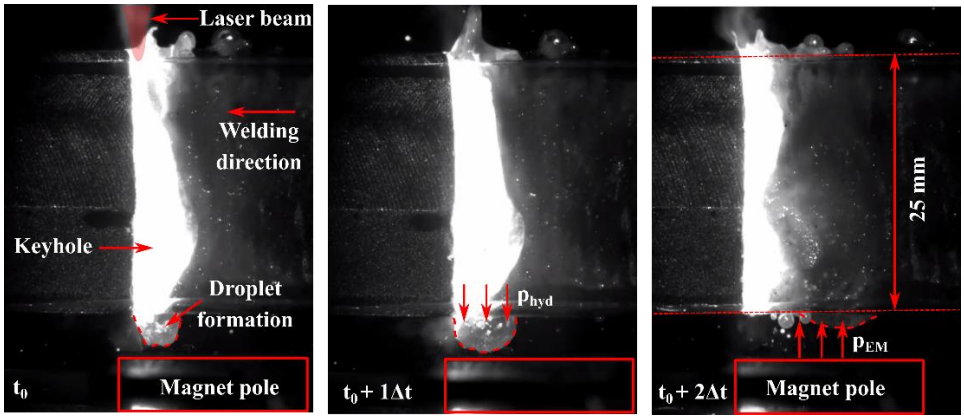

Figure 4. Highspeed images of LBW steel-glass configuration during droplet formation (left and middle) and its prevention through the electromagnetic pressure (right).

With a turn of the magnet poles 45° to the initial state, a vortex on the root part is formed due to the inhomogeneous course of the electric current and its concentration in the weld pool. By turning the magnetic field orientation, a rotational component of the Lorentz force is formed. This vortex is visible on the Figure 5. Additionally, the melt pool geometry can be recognized in terms of a liquid movement. Due to the Marangoni convection on the free surfaces the weld pool length in the top surface as well as in the root is large. The melt pool geometry can also be observed on the welded specimen, especially in the end crater area, see Figure 6. It correlates with the high-speed images and the assumption that this area actually reflects the melt pool geometry. The seam profile at the start due to the ramp time of 450 ms for the laser power from 0 kW to 18.7 kW can be seen clearly.

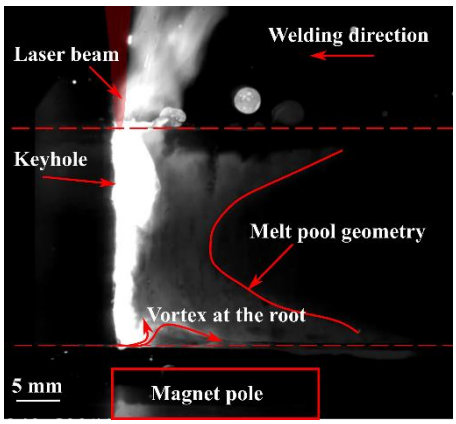

Figure 5. Melt pool geometry of LBW sample with electromagnetic support with turn of the magnetic field orientation of 45°.

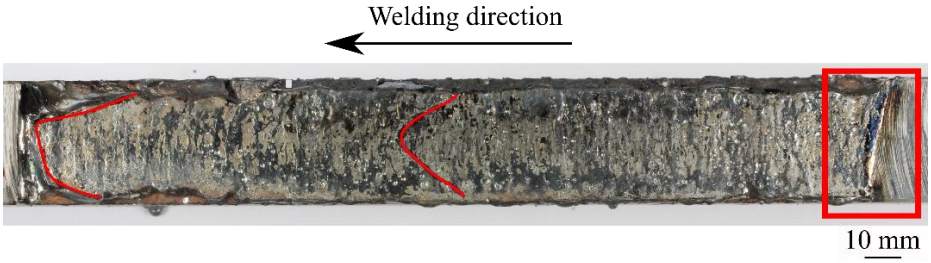

Figure 6. Laser beam welded specimen in steel-glass configuration with the marked melt pool geometry.

Figure 7 shows the velocity vectors for a sequence of LBW sample with electromagnetic support. These analyses can clearly show the flow directions and their velocities. Also, the shape of the molten pool can be estimated as a virtual transition boundary between non-zero and nearly zero displacements.

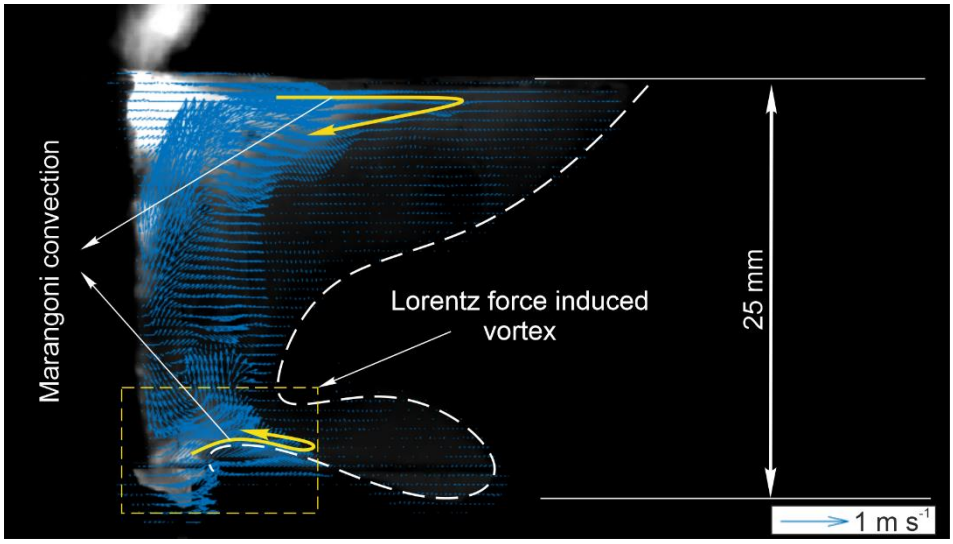

Figure 7. Velocity vectors estimated using optical flow algorithm of LBW sample with electromagnetic support with turn of the magnetic field orientation of 45°.

The velocities vary between 0.01 m s^{-1} and 1 m s^{-1} depending on the distance from the keyhole and the temperature as well as the viscosity. The flows that can be on the laser beam path e.g. on the keyhole wall have two directions, downwards and upwards. The upward and downward flows are mainly driven by the vapor velocity in the keyhole. The Marangoni flow can also be observed on the surface of the molten pool, as shown by the vectors on the surface from left to right and are marked with the yellow lines. The influence of the magnet induced Lorentz force can be observed in the weld root. A drop formation can be seen in Figure 7. The Lorentz force acts against the gravitational force and hydrostatic pressure and pushes the melt again in the weld pool. This leads to the formation of a vortex in the weld root region. It is evident, that two different vortexes are formed on the top side and weld root respectively. On the top surface, the additional elements from the powder are mixed well, where the vortex in the root leads to a material flow within the base material. As it can be seen in Figure 7, a necking region with a low melt flow velocity is formed between the two vortices. This phenomenon appears to the separation in the material transport from the top to the weld root due to the opposite vortices which are formed in the top part and root part and are separated by a necking region. The melt pool geometry correlates with the geometry in Figure 6.

As it can be seen on Figure 8, a weld-through was guaranteed and the drop-outs were prevented by the externally applied magnetic field in every case. Furthermore, the distribution of the austenitic powder

316L-Si which was filled into the prefabricated groove before welding, can be seen. For this analysis the magnetic field orientation was variated between 0° and 45° in steps of 15°. With an orientation of the magnetic field transverse to the welding direction (0°-case), the powder can be measured at a depth up to 13 mm. With a turn of the magnet poles of 15°, the depth of the mixing area decreases to 12.3 mm. For a 30° and 45°-turn of the magnetic field orientation, the depth of mixing decrease to 11.5 mm and 9.7 mm respectively. These new findings contradict with the results published in [21], where a turn of the magnetic field orientation was recommended. Although, there is vortex in the root part which may be helpful for a better mixing or homogenous distribution of the additional wire or powder, but because of the separation of the melt flow movement and the necking in between the two regions, which is described above, the effectiveness of the filler wire or powder transport to the root part is decreased. As it can be seen in Figure 7, a high vortex is formed due to the rotation of the magnetic field orientation especially in the root part. A slight vortex across the entire material thickness would be more helpful for the element transport and mixing behaviour.

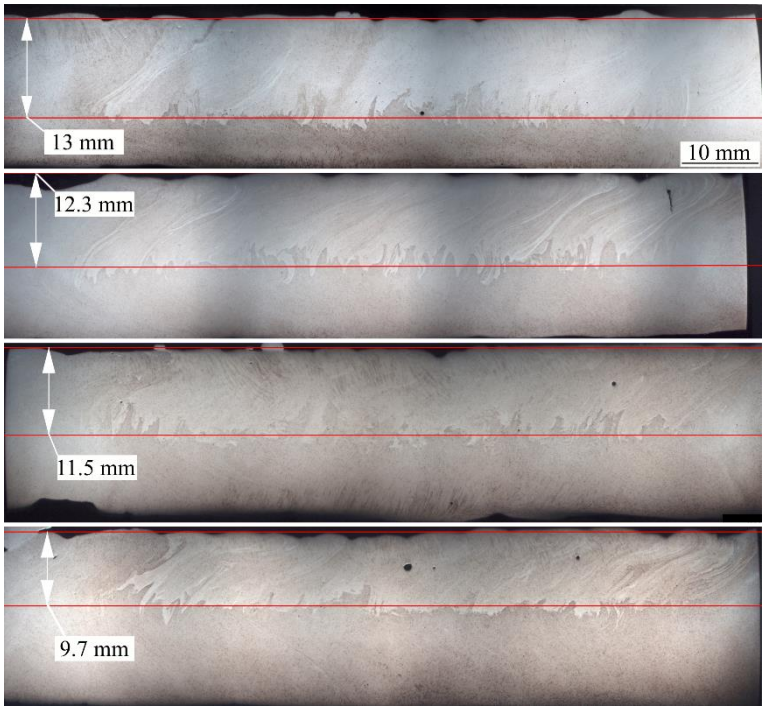

Figure 8. Longitudinal sections of the laser beam welded specimens in steel-glass configuration, filled with an austenitic powder 316L-Si: variation of the magnetic field orientation of 0°, 15°, 30° and 45° perpendicular to the welding direction (from to top to bottom).

3.2. Hybrid laser-arc welds

An example of HLAW plate with electromagnetic weld pool support is shown in Figure 9. The visual test of the welded joint did not reveal imperfections, such as incomplete fusion or lack of penetration. The root quality meets the requirements related to quality level B according to ISO 12932. A weld-through is guaranteed over the entire seam length. The AC magnet was operated with an oscillation frequency of 1.2 kHz at a power of 2.1 kW and a magnetic flux density of 157 mT.

Figure 9. The top surface and the root of the hybrid laser arc welded joint with electromagnetic weld pool support technique using 17.7 kW laser power and 9.8 kW arc power at a welding speed of 1.3 m min^{-1}.

The influence of the oscillation frequency on the element mixing was investigated. Therefore, the magnetic field orientation was turned 30° transverse to the welding direction and the frequency was variated between 0.8 kHz, 1.2 kHz and 1.7 kHz. According to the skin layer theory, the oscillating frequency has a major influence on the depth, where the magnetic field and the induced eddy currents have an impact on the melt flow. With increasing oscillation frequency, the skin layer depth decreases where a strong Lorentz force is formed in a thin layer. With decreasing oscillation frequency, the filler wire mixing was improved as the formed Lorentz forces are distributed over the entire thickness of the plate. A homogenous distribution of the additional filler wire is reached to a depth of approx. 16 mm. It is known that with decreasing oscillating frequency the skin layer depth increases. For a frequency of 800 Hz, the estimated skin layer depth corresponds to 20.5 mm and reaches the entire seam thickness, so that a better mixing takes place. The results of the Ni distribution over the entire seam thickness by a turn of the magnetic field orientation of 30° and variation of the oscillating frequency are shown in Figure 10.

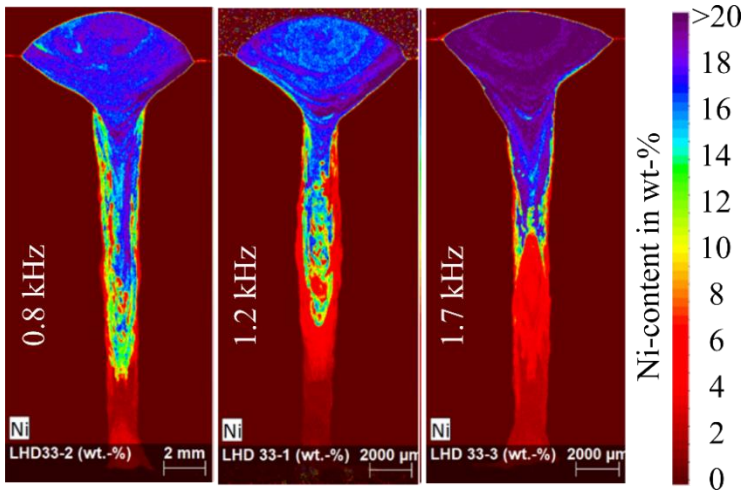

Figure 10. Ni distribution of a single-pass HLAW with electromagnetic weld pool support by a turn of the magnetic field orientation of 30° and variation of the oscillating frequency, measured by XRF

4. Conclusion

Full penetration LBW in steel-glass configuration for 25 mm thick S355J2 were performed for different designs of the orientation of the external oscillating magnetic field. Thereby, high-speed images were taken with a high-speed camera. The formation of the drop-outs on the weld seam root and their prevention due to the electromagnetic pressure provided with an AC magnet could be recorded. The root

quality could be classified in the highest evaluation group B according to EN ISO 12932. By turning the magnetic field, a rotational component of the Lorentz force was generated, which forms a strong vortex in the weld seam root. The velocity vectors were estimated using an optical flow algorithm and confirm the vortex in the root. Nevertheless, a strong vortex in the root was not helpful for a better mixing of the additional austenitic powder throughout the entire seam thickness. However, the oscillating frequency shows a high impact on the mixing behaviour due to the change of the skin layer depth. A low frequency of just 0.8 kHz was helpful to transport the filler wire into the seam root part at HLAW of 20 mm thick S355J2 plates.

Funding
The research project was carried out in the framework of the Industrial Collective Research programme (IGF No.20.827N). It was supported by the Federal Ministry for Economic Affairs and Energy (BMWi) through the AiF (German Federation of Industrial Research Associations e.V.) based on a decision taken by the German Bundestag. Financial funding is gratefully acknowledged.

ORCID iDs
Ö. Üstündağ https://orcid.org/0000-0002-7352-429X
N. Bakir https://orcid.org/0000-0001-6847-0365
A. Gumenyuk https://orcid.org/0000-0002-8420-5964

M. Rethmeier https://orcid.org/0000-0001-8123-6696References

[1] Üstündag Ö, Avilov V, Gumenyuk A and Rethmeier M 2018 *J. Phys.: Conf. Ser.* **1109** 012015
[2] Wahba M, Mizutani M and Katayama S 2016 *Mater. Des.* **97** 1
[3] Rethmeier M, Gook S, Lammers M and Gumenyuk A 2009 *Q. J. Jpn. Weld. Soc.* **27** 74
[4] Katayama S, Yohei A, Mizutani M and Kawahito Y 2011 *Phys. Procedia* **12** 75
[5] Reisgen U, Olschok S and Longerich S 2010 *Proceedings of 29th International Congress on Applications of Lasers & Electro-Optics ICALEO* Anaheim USA, 638
[6] Reisgen U, Olschok S and Jakobs S 2016 *Phys. Procedia* **56** 653
[7] Zhang C, Li G, Gao M and Zeng X 2017 *Materials* **10** 106
[8] Frostevarg J and Heussermann T 2015 *The IIW International Conference on High Strength Materials–Challenges and Applications* Helsinki Finland
[9] Avilov V, Gumenyuk A, Lammers M and Rethmeier M 2012 *Sci. Technol. Weld. Join.* **17** 128
[10] Üstündağ Ö, Gook S, Gumenyuk A and Rethmeier M 2018 *Procedia Manuf.* **36** 112
[11] Gook S, Gumenyuk A and Rethmeier M 2014 *Sci. Technol. Weld. Join.* **19** 15
[12] Bunaziv I, Wenner S, Ren X, Frostevarg J, Kaplan A F and Akselsen O M 2020 *J. Manuf. Process.* **54** 228
[13] Karhu M, Kujanpaa V, Gumenyuk A and Lammers M 2013 *Proceedings of 32nd International Congress on Applications of Lasers & Electro-Optics ICALEO* Miami USA252
[14] Sohail M, Karhu M, Na S J, Han S W and Kujanpaa V 2017 *J. Laser Appl.* **29** 042009
[15] Zhao L, Sugino T, Arakane G and Tsukamoto S 2009 *Sci. Technol. Weld. Join.* **14** 457
[16] Suder W, Ganguly S, Williams S and Yudodibroto B Y 2021 *J. Mater. Process. Technol.* **291** 117040
[17] Gatzen M, Tang Z and Vollertsen F 2011 *Phys. Procedia* **12** 56
[18] Tang Z and Gatzen M 2010 *Phys. Procedia* **5** 125
[19] Vollertsen F and Thomy C 2006 *J. Laser Appl.* **18** 28
[20] Meng X, Bachmann M, Artinov A and Rethmeier M 2021 *J. Mater. Process. Technol.* **294** 117135
[21] Üstündağ Ö, Avilov V, Gumenyuk A and Rethmeier M 2019 *Metals* **9** 594